Random Access Compressed Sensing over Fading and Noisy Communication Channels

Fatemeh Fazel, Maryam Fazel, and Milica Stojanovic

***Abstract*—Random Access Compressed Sensing (RACS) is an efficient method for data gathering from a network of distributed sensors with limited resources. RACS relies on integrating random sensing with the communication architecture, and achieves overall efficiency in terms of the energy per bit of information successfully delivered. To address realistic deployment conditions, we consider data gathering over a fading and noisy communication channel. We provide a framework for system design under various fading conditions, and quantify the bandwidth and energy requirements of RACS in fading. We show that for most practical values of the signal to noise ratio, energy utilization is higher in a fading channel than it is in a non-fading channel, while the minimum required bandwidth is lower. Finally, we demonstrate the savings in the overall energy and the bandwidth requirements of RACS compared to a conventional TDMA scheme. We show that considerable gains in energy -on the order of 10 dB- are achievable, as well as a reduction in the required bandwidth, e.g., 2.5-fold decrease in the bandwidth for a network of 4000 nodes.**

***Index Terms*—Wireless network, random access, compressed sensing, fading, Rayleigh, Ricean, log-normal shadowing.**

I. Introduction

WIRELESS sensor network technology has enabled affordable large coverage and long term monitoring of the natural environment [1] such as ocean observation [2], monitoring volcanic eruptions [3] and long term studies of the glaciers [4] which help our understanding of the climate change. Such applications require the least control and intervention as well as minimum energy consumption. The data from distributed sensors is conveyed to a fusion center (FC) where a full map of the sensing field is reconstructed. Once the network is deployed, there can be little access to the sensors, hence re-charging the batteries is difficult. This is especially of concern in underwater networks, where sensor nodes are hundreds of meters below the surface, or in hostile environments where access to the sensor nodes is prohibited. Data gathering is further exacerbated in situations where bandwidth is constrained and the communication channel introduces distortion. Long term deployment of sensor networks in such environments calls for the integration between sensing, communication, and field recovery.

Manuscript received April 5, 2012; revised September 10, 2012; accepted November 21, 2012. The associate editor coordinating the review of this paper and approving it for publication was S. Valaee.

Research funded in part by ONR grant N00014-09-1-0700, NSF grant 0831728, and NSF CAREER grant ECCS-0847077.

F. Fazel and M. Stojanovic are with the Department of Electrical and Computer Engineering, Northeastern University, Boston, MA, 02115, USA (e-mail: {ffazel, millitsa}@ece.neu.edu).

M. Fazel is with the Department of Electrical Engineering, University of Washington, Seattle, WA, 98195, USA (email: mfazel@u.washington.edu).

Digital Object Identifier 10.1109/TWC.2013.032013.120489

Application of compressed sensing in wireless sensor networks was first introduced in [5]–[7], where the authors use phase-coherent analog transmission of randomly-weighted data from sensor nodes to the FC. The additive property of the multiple-access channel then allows for attaining projections of data onto an appropriate basis at the FC. A number of references use compressed sensing techniques in wireless sensor networks to recover phenomena that are sparse in the spatial domain, e.g., event detection [8], or tracking multiple targets [9]. In [10], the authors consider a data gathering scheme where weighted sums of sensor data, which are combined while being relayed, are delivered to the FC. Authors in [11] use adaptive compressed sensing to find the projection vector that strikes a balance between information gain and energy consumption. Using an estimation of signal statistics, the authors in [12], [13] propose a protocol for data recovery which combines compressed sensing and principal component analysis (PCA), with the latter providing the sparsity basis. To reduce the cost of collecting measurements, [14] proposes that projections are formed over clusters of neighboring sensors. The feature distinguishing our work from the existing literature is the integration of the communication and channel access considerations into the design of data acquisition.

In [15], [16] we proposed an integrated sensing and communication architecture referred to as *Random Access Compressed Sensing* (RACS), which achieves overall efficiency in terms of the energy per bit of information successfully delivered to the FC. Considering the fact that most natural phenomena have a sparse representation in an appropriate domain (e.g., the spatial-frequency domain), RACS capitalizes on integrating compressed sensing with random channel access. The former supports transmission of sensor data from only a random subset of all the nodes, thus reducing the overall energy consumption, while the latter supports a robust and simple implementation that eliminates the need for synchronization, scheduling, and downlink feedback. In the present paper, we address realistic deployment conditions, that include fading and noisy communication channels. Inclusion of channel imperfections affects the data collection process, and we thus analyze their effect on the total number of packets collected. We provide network design principles for such channels, and analyze the network performance in terms of the energy and bandwidth required for successful field recovery. The novelty of the current work lies in providing theoretical analysis of communication aspects of the RACS scheme, thus bringing it closer to realistic deployment conditions.

The rest of the paper is organized as follows. In Section II, we provide an overview of the principles of RACS. In Sec-

TABLE I
LIST OF THE SYMBOLS

symbol	definition
N	size of the signal/network
S	sparsity
T	collection interval
T_{coh}	coherence time of the process
γ	instantaneous SINR
P_{ss}	probability of sufficient sensing
p_s	probability of packet success
B_s	minimum bandwidth requirement
$E_{\min}$	minimum energy consumption

tion III, we study successful packet detection in the presence of channel fading and communication noise and in Section IV, we evaluate system performance under Ricean, Rayleigh and Lognormal fading conditions. Section V outlines the design methodology. In Section VI, we study the bandwidth and energy utilization of the network. Finally, we provide concluding remarks in Section VII. A summary of the symbols used in this paper is provided in Table I.

II. RACS: RANDOM ACCESS COMPRESSED SENSING

The theory of compressed sensing [17], [18] establishes that if a signal of dimension N has an S-sparse representation in an appropriate domain $\mathbf{\Psi}$ (referred to as the sparsity basis), it can be recovered, with very high probability, from $\mathcal{O}(\nu S \log N)$ random measurements obtained in a sensing domain $\mathbf{\Phi}$. The coefficient ν represents the coherence between the sparsity basis $\mathbf{\Psi}$ and the sensing basis $\mathbf{\Phi}$ and is defined as [18]

$$\nu(\mathbf{\Phi}, \mathbf{\Psi}) = \sqrt{N} \max_{1 \le k,j \le N} |\langle \mathbf{\Phi}_k, \mathbf{\Psi}_j \rangle| \tag{1}$$

Consider a sensor network where $N = IJ$ sensors are placed on a grid, with J and I sensors in x and y directions, respectively. At time t, the sensor node located at coordinate (i, j) acquires a measurement $u_{ij}(t)$. This process has a coherence time T_{coh}, such that $u_{ij}(t_1) \approx u_{ij}(t_2)$ for $|t_1 - t_2| \le T_{coh}$. In what follows we focus on an observation window of size $T \le T_{coh}$, dropping the time index from the sensor measurements. The measurements are sent to the FC, where the gathered data are used to build a map of the sensing field (e.g., a geographical, chemical, or a temperature map), denoted by

$$\mathbf{U} = [u_{ij}]_{\substack{i=1,\ldots,I \\ j=1,\ldots,J}} \tag{2}$$

Many natural signals have a compressible (sparse) representation in the frequency domain,[1] i.e., assuming $\mathbf{u} = \mathrm{vec}(\mathbf{U})$, the vector $\mathbf{v} = \mathbf{\Psi}^{-1}\mathbf{u}$ is sparse, where $\mathbf{\Psi^{-1}}$ represents the DFT transform matrix. In more details, let $\mathbf{V} = \mathbf{W}_I \mathbf{U} \mathbf{W}_J$ represent the two-dimensional spatial discrete Fourier transform of $\mathbf{U}$, where $\mathbf{W}_I$ is the matrix of discrete Fourier transform coefficients, $\mathbf{W}_I[m,k] = \frac{1}{\sqrt{I}} e^{-j2\pi mk/I}$. It can be shown that

$$\mathbf{v} = (\mathbf{W}_J \otimes \mathbf{W}_I)\mathbf{u} \tag{3}$$

[1]In some cases there may exist bases other than the Fourier, in which the natural signal has an even sparser representation. Without loss of generality, here we will focus on sparse Fourier representations, while providing a general setup encompassing any appropriate basis.

where $\mathbf{v} = \mathrm{vec}(\mathbf{V})$. Noting that $\mathbf{\Psi} = (\mathbf{W}_J \otimes \mathbf{W}_I)^{-1}$, it follows that

$$\mathbf{v} = \mathbf{\Psi}^{-1}\mathbf{u}. \tag{4}$$

We note that the spatial coordinate basis and the spatial frequency basis are maximally incoherent, i.e., the coherence between the (spatial) Fourier domain $\mathbf{\Psi}$ and the spatial domain $\mathbf{\Phi}$ is $\nu(\mathbf{\Psi}, \mathbf{\Phi}) = 1$ (see [19]).

RACS thus works as follows: The sensor node at coordinate (i, j) on the grid measures the signal of interest u_{ij} at random time instants within T, independently of the other nodes, at a rate of λ_1 measurements per second. It then encodes each measurement along with the node's location tag into a packet of L bits, which is then modulated and transmitted to the FC in a random access fashion. Because of the random nature of channel access, packets from different nodes may create interference at the FC, or they may be distorted because of noise. A packet is declared erroneous if it does not pass the cyclic redundancy check (CRC) or a similar verification procedure. Motivated by the compressed sensing principle, the key idea in RACS is to let the FC simply discard the erroneous packets, since the FC does not care which specific sensors are selected as long as (i) the selected subset is chosen uniformly at random, and (ii) there are sufficiently many useful packets remaining to allow for the reconstruction of the field.

The FC thus discards the packets that are erroneous and collects the remaining useful packets over an observation interval T. The interval T is assumed to be shorter than T_{coh}, such that the process can be approximated as fixed during one such interval. By the end of the observation interval, the useful data at the FC can be expressed as

$$\mathbf{y} = \mathbf{R}\mathbf{u} + \mathbf{z} \tag{5}$$

where $\mathbf{z}$ represents the sensing noise and $\mathbf{R}$ models the selection of the correct packets. Specifically, $\mathbf{R}$ is a $K \times N$ matrix with K corresponding to the number of useful measurements collected during T. The rows of the matrix $\mathbf{R}$ can be regarded as K rows of an $N \times N$ identity matrix, picked uniformly at random, i.e., each row consists of a single 1 in the position corresponding to the sensor contributing the useful packet. The FC can form the matrix $\mathbf{R}$ from the correctly received packets, since they carry the location tag.

We emphasize the distinction between the *sensing noise* $\mathbf{z}$, which arises due to the limitations in the sensing devices, and the *communication noise*, which is a characteristic of the transmission system. The sensing noise appears as an additive term in Eq. (5), whereas the communication noise results in packet errors and its effect is captured in the matrix $\mathbf{R}$. In addition to communication noise, fading also affects packet detection and similarly affects the number of rows of the matrix $\mathbf{R}$, as will be discussed in Section III.

Noting that $\mathbf{u} = \mathbf{\Psi}\mathbf{v}$, where $\mathbf{\Psi}$ is the inverse Discrete Fourier Transform matrix, Eq. (5) can be re-written in terms of the sparse vector $\mathbf{v}$ as

$$\mathbf{y} = \mathbf{R}\mathbf{\Psi}\mathbf{v} + \mathbf{z} \tag{6}$$

Ignoring the sensing noise $\mathbf{z}$, in order to reconstruct the map of the field, the FC recovers $\mathbf{v}$ by solving the following

minimization problem:

$$\text{minimize}_{\tilde{\mathbf{v}}} \ \|\tilde{\mathbf{v}}\|_{\ell_1} \quad \text{subject to } \mathbf{R}\boldsymbol{\Psi}\tilde{\mathbf{v}} = \mathbf{y}. \tag{7}$$

The theory of compressed sensing (specifically, [17]) states that as long as the number of observations, picked uniformly at random, is greater than $N_s = CS\log N$, then with very high probability the solution to the convex optimization problem (7) is unique and is equal to $\mathbf{v}$. Thus, it suffices to ensure that the FC collects a minimum number of packets, $N_s = CS\log N$, picked uniformly at random from different sensors, to guarantee accurate reconstruction of the field with very high probability. Note that C is a constant that is independent of S and N.[2]

Note that the results in this paper are not restricted to the grid model and can be extended to the cases where the sensors are either placed on a nonuniform rectangular grid, or placed non-uniformly on parallel lines. In such scenarios, the Fourier representation is replaced by the two-dimensional nonuniform discrete Fourier transform [20].

III. Packet Detection in Fading and Noise

A packet is either detected successfully, hence contributes to forming Eq. (6) at the FC, or is corrupted as a result of collisions or channel imperfection, hence discarded. In this section, we model the procedure to form Eq. (6), i.e., the procedure to determine the matrix $\mathbf{R}$ or more specifically, the number of correct packets and their corresponding location.

A wireless communication channel is typically modeled by a distance-dependent propagation loss, shadowing, and small-scale fading. Let $L(d_i)$ represent the attenuation or path loss, which depends on the distance d_i between the sensor generating packet i and the FC. Since the network is stationary, each node can be equipped with the knowledge of its distance to the FC, which remains unchanged throughout the data collection interval. Each node can thus compensate for the path loss $L(d_i)$ by adjusting its transmission power. This ensures that the packets from all the nodes arrive at the FC at the same nominal power P_0. The total channel gain c_i, observed by the i-th packet, is thus modeled as

$$c_i = e^{g_i} h_i \tag{8}$$

where $g_i \sim \mathcal{N}(0, \sigma_g^2)$ models the large-scale lognormal shadowing and $h_i \sim \mathcal{CN}(\overline{h}, \sigma_h^2)$ models the small-scale fading. We assume a quasi-static fading model in which the channel coefficient c_i is fixed for the duration of a packet T_p, and changes independently from one packet to the next. This is a reasonable assumption since the packets generated by a single node are transmitted at a relatively low rate, i.e., they are distanced sufficiently apart in time such that they undergo independent fades. We also assume that the colliding packets undergo uncorrelated channels. This is a fair assumption because the colliding packets are not likely to be from neighboring nodes.[3]

In the absence of channel fading and communication noise, packet loss in RACS is caused by collisions, i.e., an overlap in the arrival time of two packets, which results in the loss of both packets [15], [21]. When fading is present, the situation is somewhat changed since not every collision has to result in packet loss. Namely, it is possible that although two (or more) packets overlap at the FC, one is sufficiently stronger so that it can be successfully detected. Below we discuss the probability of successful reception.

A. Interference Model

The received signal at the FC is given by

$$v_n(t) = c_0 u_0(t) + i_n(t) + w(t) \tag{9}$$

where $u_0(t)$ is the desired signal, $i_n(t)$ is the interference and $w(t)$ is the additive white Gaussian noise with power $N_0 B$, where B is the bandwidth. The interfering term can be expressed as

$$i_n(t) = \sum_{i=1}^{n} c_i u_i(t - \tau_i) \tag{10}$$

where $u_i(t)$ is the i-th interferer's signal, τ_i is the difference in the arrival times of the interfering signal with respect to the signal of interest, and the number of interfering packets n is a random variable with probability distribution $P(n)$. Assuming that packet arrivals follow a Poisson distribution, we have that

$$P(n) = \frac{(2N\lambda_1 T_p)^n}{n!} e^{-2N\lambda_1 T_p} \tag{11}$$

where $T_p = L/B$ is the packet duration.[4]

For a given node, let $X_0 = |c_0|^2 P_0$ represent the power of the desired packet, and I_n represent the total interference power. We assume that X_0 and I_n follow the probability distributions f_X and f_I, respectively. The instantaneous signal to interference and noise ratio (SINR) is given by

$$\gamma = \frac{X_0}{I_n + N_0 B} \tag{12}$$

In the worst case scenario, the packet arrivals are synchronous, i.e., $\tau_i = 0$ for $i \in \{1, \ldots, N\}$. The interference power is then given by $I_n = \sum_{i=1}^{n} |c_i|^2 P_0 = Y_n$, which follows a probability distribution f_Y. This situation, however, represents a pessimistic scenario since packet transmissions in RACS are not synchronized. Rather than considering various scenarios for the overlapping of packets, we employ a simplified model in which we assume that the strongest interferer dominates the term $i_n(t)$ [22], i.e., we assume that the interference power is $I_n = max_{i\in\{1,\ldots,n\}}|c_i|^2 P_0 = M_n$, which has a probability distribution f_M. Specifically,

$$f_M(z) = nF_X(z)^{n-1} f_X(z) \tag{13}$$

[2]If the signal has a sparse representation in a basis $\boldsymbol{\Psi}'$ other than the Fourier basis, RACS is still applicable with the condition that the number of required measurements is now adjusted to $N_s = C'\nu^2(\boldsymbol{\Phi}, \boldsymbol{\Psi}')S\log N$ where $\boldsymbol{\Phi}$ is the spatial domain and C' is a constant.

[3]Assuming a Poisson packet arrival model with per node parameter λ_1, the probability of packet collision is given by $1 - e^{-2N\lambda_1 T_p}$, where the size of the network N is large. Let us assume that each node has N_1 neighbors where $N_1 \ll N$. The probability that the packets from two neighboring nodes collide is then given by $1 - e^{-2N_1\lambda_1 T_p}$. Thus the possibility that the colliding packets originated from neighboring nodes is relatively small, i.e., $\frac{1-e^{-2N_1\lambda_1 T_p}}{1-e^{-2N\lambda_1 T_p}} \approx \frac{N_1}{N} \ll 1$.

[4]Throughout this paper we use bandwidth and bit rate interchangeably.

where $F_X(x)$ is the cumulative distribution function of X_0.

Thus we have two methods to model the interfering power,

$$I_n = \begin{cases} Y_n = \sum_{i=1}^{n} |c_i|^2 P_0 & \text{(model a)} \\ M_n = \max_i |c_i|^2 P_0 & \text{(model b)} \end{cases} \tag{14}$$

Model (a) assumes the worst case scenario, leading to an overestimation of the effect of interference and thus slightly pessimistic results for the probability of successful reception. In contrast, model (b) underestimates the effect of the interference, resulting in a probability of success that is slightly greater than the one predicted using model (a). The models (a) and (b) given by (14) thus provide upper and lower bounds, respectively, on the actual interfering power.

B. Probability of Successful Reception: Outage Model

For a given number of interfering packets n, we employ the outage model to describe the probability of successful reception $p_{s|n}(\gamma)$. In this model, $p_{s|n}(\gamma)$ is described by a step function as

$$p_{s|n}(\gamma) = \begin{cases} 0, & \gamma < b \\ 1, & \gamma \geq b \end{cases} \tag{15}$$

The effects of coding, modulation and other system parameters are implicit in one parameter $b > 1$,[5] which is a predefined threshold with a typical value $b = 2 - 6$ [23], [24].[6]

Under the outage model, averaging $p_{s|n}(\gamma)$ over the fading statistics results in (see Appendix A)

$$p_{s|n} = \begin{cases} \int_{bN_0B}^{\infty} f_X(x)dx & \text{for } n = 0 \\ \int_b^{\infty} \int_{N_0B}^{\infty} f_X(\gamma w) f_I(w - N_0B) w dw d\gamma & \text{for } n \geq 1 \end{cases} \tag{17}$$

where $f_I = f_Y$ for model (a) and $f_I = f_M$ for model (b). The total probability of successful reception is then given by

$$p_s = \sum_{n=0}^{N} P(n) p_{s|n} \tag{18}$$

Small-scale fading, modeled by h_i in Eq. (8), creates relatively fast variations in the channel, and is thus responsible for short term signal variations. Shadowing, on the other hand, occurs over longer time scales, creating slow variations in the mean signal amplitude. Several different models for the probability distribution of a composite multipath/shadowed environment have been proposed, among which are the composite Gamma/lognormal and the Suzuki models [26], [27]. In most environments, however, either shadowing or multipath fading is the dominant factor. In what follows, we proceed to investigate the probability of successful reception under Ricean, Rayleigh and log-normal fading statistics.

[5]Note that if multi-user detection techniques are employed, the value of b may be smaller than 1. In this paper we assume a single-user detector.

[6]As an alternative to the outage model, we can use the BER model. Treating interference as Gaussian noise, we can use the bit error probability $p_b(\gamma)$ to determine the probability of receiving a correct packet as

$$p_{s|n}(\gamma) = (1 - p_b(\gamma))^L \tag{16}$$

Using powerful long codes, Eq. (16) approaches a step function, thus $p_{s|n}(\gamma)$ in the BER model approaches that in the outage model [25].

IV. Fading Scenarios

A. Small-scale Fading: Ricean and Rayleigh models

In propagation environments where the data collection interval T is short compared to the de-correlation interval of the shadowing, the variation in shadowing can be assumed negligible. The effects of path loss and shadowing, included in a gain $G_i = L(d_i)e^{g_i}$, can thus be pre-compensated at the transmitter by means of a power control mechanism, i.e., the transmitter adjusts its power to P_0/G_i^2. The power control can be achieved by an occasional downlink beacon which enables the sensor node to estimate the shadowing coefficient. Thus, only small scale fading remains in model (8).

The distribution of the amplitude of the channel $R_i = |h_i|$ in Ricean fading is given by

$$f_{R_i}(r_i) = 2(K+1) r_i \exp\left(-r_i^2(K+1) - K\right) I_0\left(2\sqrt{K(K+1)} r_i\right) \tag{19}$$

where K is the Ricean factor (defined as the ratio of the power in the specular component to the power in the scattered component), where we assume that the sum power in both components is normalized to one, and $I_0(\cdot)$ is the zero-order modified Bessel function of the first kind. In a Ricean fading channel, the probability of successful reception, given by Eq. (17), can be evaluated numerically using the distributions $f_X(x)$, $f_Y(y)$ and $f_M(z)$ provided in the Appendix B.

In the special case when there is no LOS component present, i.e., when $K = 0$, the envelope of h_i follows a Rayleigh distribution. In this case, the distribution of X_0 is exponential,

$$f_X(x) = \frac{1}{P_0} e^{-x/P_0} \quad x \geq 0 \tag{20}$$

For model (a), the interference power Y_n follows a gamma distribution

$$f_Y(y) = \frac{1}{P_0} \frac{(y/P_0)^{n-1}}{(n-1)!} e^{-y/P_0} \tag{21}$$

and for the interference model (b) we have that

$$f_M(z) = \frac{n}{P_0} \left(1 - e^{-z/P_0}\right)^{n-1} e^{-z/P_0} \tag{22}$$

Defining $\gamma_0 = P_0/N_0B$, the probability of successful reception is obtained in closed form as

$$p_s = e^{-b/\gamma_0} e^{-2N\lambda_1 T_p \frac{b}{1+b}} \tag{23}$$

and

$$p_s = e^{-b/\gamma_0} e^{-2N\lambda_1 T_p} \left(1 + \sum_{n=1}^{N-1} \frac{(2N\lambda_1 T_p)^n}{n!} \sum_{i=0}^{n} \binom{n}{i} \frac{(-1)^i}{1 + i/b}\right) \tag{24}$$

for models (a) and (b), respectively. In a non-fading channel, provided that $\gamma_0 \geq b$, p_s corresponds to the probability of no collision [15]. Also, in a noiseless fading channel, the probability of successful reception reduces to $p_s = e^{-2N\lambda_1 T_p \frac{b}{b+1}}$ [28].

1) Numerical Examples: We now provide numerical results to demonstrate the impact of small scale fading on the probability of successful reception. Unless otherwise noted,

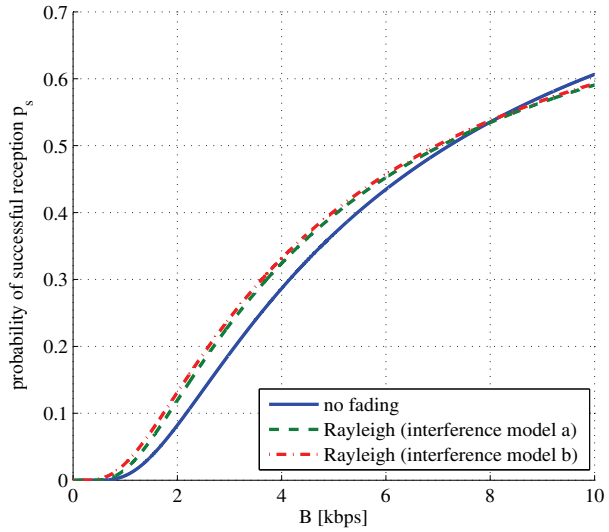

Fig. 1. Probability of successful reception p_s versus the bandwidth B for a Rayleigh fading channel. Both interference models (a) and (b), corresponding to a lower and an upper bound on the actual p_s are shown. The gap between the two interference models (a) and (b) decreases as bandwidth grows.

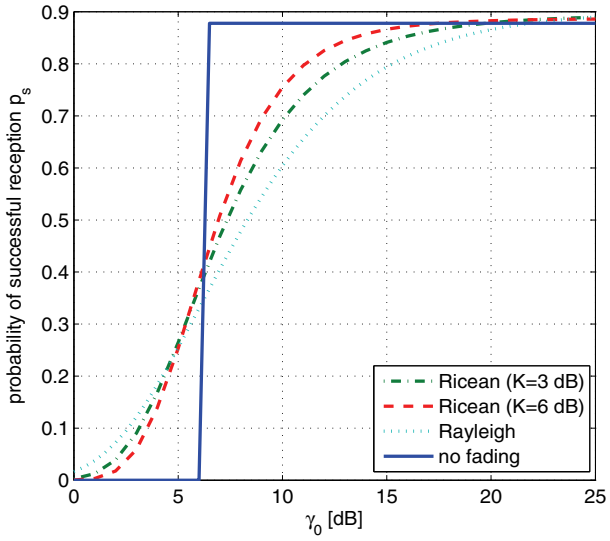

Fig. 2. Probability of successful reception versus γ_0, for $B = 38.4$ kbps over a Ricean fading channel with $K = 3$ and $K = 6$ dB, as well as Rayleigh and non-fading channels. (The value of the bandwidth used corresponds to the Mica2 sensors used in environmental monitoring networks: www.xbow.com).

we employ the following system parameters in our numerical examples: $N = 2500$ nodes, $L = 1000$ bits per packet, $\lambda_1 = 10^{-3}$ packet/sec and $b = 4$.

Fig. 1 shows the probability of successful reception in Rayleigh fading (i.e., when $K = 0$) using the two models (a) and (b) for interference given by Eqs. (23) and (24), respectively. As expected, model (b) predicts a larger p_s than model (a). We note that for our choice of system parameters, the bounds on p_s, provided by models (a) and (b), are tight, and the gap further diminishes as bandwidth is increased. Thus, the actual p_s is approximated relatively accurately by each model. Throughout the rest of the paper, unless otherwise noted, we use model (a) and design the system for the worst case scenario, keeping in mind that the actual system performance will be slightly better than assumed by this model. We also note from Fig. 1 that for small bandwidths, fading boosts the probability of successful reception. The reason is that for smaller B, the probability of packet overlap is larger (due to longer packet duration T_p). When fading is present, not all packet collisions result in packet loss. Namely, although two or more packets overlap at the FC, one may be sufficiently stronger such that it can be detected successfully. When bandwidth is increased, the probability of packet overlaps reduce and the aforementioned benefit fades. As a matter of fact, the fluctuations in the SNR due to fading may reduce the SNR below the detection threshold b and hence fading in the large bandwidth scenario will deteriorate the probability of success.

Fig. 2 shows p_s in a Ricean fading channel for $K = 3$ and $K = 6$ dB as well as in a Rayleigh fading channel. In a non-fading channel, when $\gamma_0 < b$, due to the high noise level, packets are not successfully detected. In this scenario the fluctuations of the received power due to fading may raise the SNR above the threshold b, hence boosting the probability of successful detection. We observe that fading enhances the probability of successful reception in two regimes: 1) when noise is dominant (i.e., when γ_0 is small), meaning that most packet losses are caused by noise, and 2) when noise is small and interference is dominant, i.e., most packet losses are due to collisions. In both cases, fading boosts the performance by turning some instances of packet loss into successful receptions. In other scenarios, fading deteriorates the performance.

Finally, Fig. 3 shows p_s versus the Rice factor K. We have considered two scenarios: Fig. 3(a) shows p_s for $\gamma_0 = 15$ dB. In this noise regime, the success rate is lower in fading, as also shown in Fig. 2. Fig. 3(b) shows p_s for $\gamma_0 = 30$ dB. In this scenario, most packet losses are a result of collisions (and not noise), for which fading enhances the success rate. As expected, the Ricean and Rayleigh fading scenarios converge when $K = 0$, and as K increases p_s in a Ricean fading channel approaches that in a non-fading channel.

B. Log-normal Shadowing

When the packet duration T_p is long compared to the shadowing time-scale, the receiver can average out the effects of small-scale fading. Thus the communication system performance will only depend on the log-normal shadowing, i.e., the slow variations of the mean signal. It is shown that in an urban land mobile environment, de-correlation of log-normal shadowing occurs on time-intervals on the order of 7-13 seconds [29]. Thus, when T_p is on the order of a few seconds (i.e., when B is small), the small-scale fading can be averaged out. The pdf of the received power of a packet can then be modeled as

$$f_X(x) = \frac{1}{\sqrt{2\pi\sigma^2}x} e^{-(\log x)^2/2\sigma^2} \tag{25}$$

where $\sigma = 2\sigma_g$, with σ_g denoting the standard deviation of g_i in Eq. (8). The dB spread of the channel is defined as $\sigma_{dB} =$

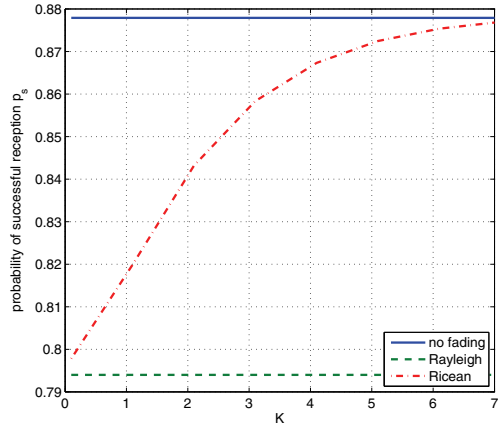

(a) $\gamma_0 = 15$ dB

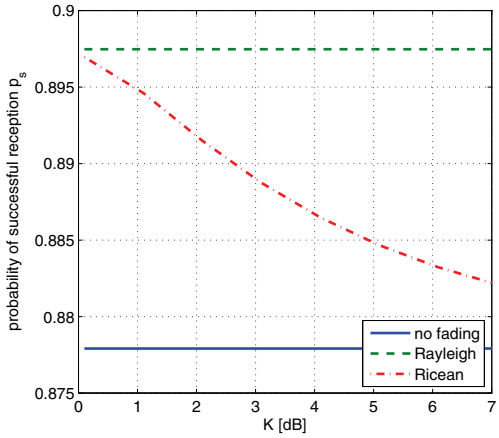

(b) $\gamma_0 = 30$ dB

Fig. 3. Probability of successful reception p_s versus the Rice factor K, for $B = 38.4$ kbps. As expected, the Ricean and Rayleigh scenarios converge when $K = 0$. As K increases, the probability of successful reception in Ricean fading approaches that of the non-fading channel. Note that as shown in Fig. 2, for $\gamma_0 = 15$ dB, fading deteriorates the probability of successful reception, whereas for $\gamma_0 = 30$ dB (large SNR regime) fading boosts p_s.

$(10/\log 10)\sigma$, which, in practice, takes on values between $6-12$dB [30]. The pdf of the interference power in model (b) is determined as

$$f_M(z) = nQ\left(\frac{-\log z}{\sigma}\right)^{n-1} \frac{1}{\sqrt{2\pi\sigma^2 z}} e^{-(\log z)^2/2\sigma^2} \quad (26)$$

In order to determine the pdf of the interference power in model (a), we note that the sum of log-normal random variables can be approximated as a log-normal, i.e.,

$$f_Y(y) = \frac{1}{\sqrt{2\pi\sigma_n^2 x}} e^{-(\log x - m_n)^2/2\sigma_n^2} \quad (27)$$

The parameters m_n and σ_n depend on the number of interfering packets n, and can be approximated using several different methods [31]–[33]. The probability of successful packet reception can now be evaluated numerically using (17), and either models (26) or (27).

Fig. 4 shows the probability of successful reception under model (b) compared with that under model (a). For model (a) we use the Wilkinson's, the Fenton's, and the Schwartz-Yeh's

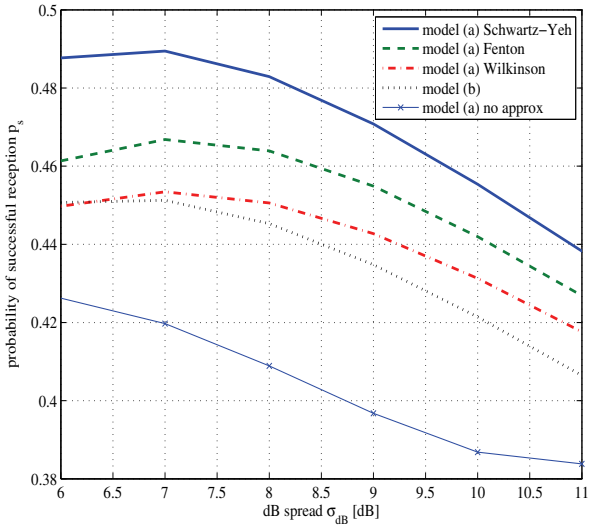

Fig. 4. Probability of successful reception p_s in log-normal shadowing. For interference model (a), Schwartz and Yeh's [31], Fenton's [32] and Wilkinson's [33] methods are considered. We note that compared to our model (b), the approximations used in model (a) do not yield sufficient accuracy to be used in predicting the probability of success. Thus, in case of log-normal shadowing, we abandon model (a) and use model (b) instead. For comparison, we also plot the results corresponding to model (a) when no approximations are used, i.e., when we numerically evaluate the sum of lognormal random variables.

methods to determine m_n and σ_n. All of these methods rely on approximating the sum to be log-normally distributed, but use different approximation techniques. For comparison, we also plot model (a) when no approximations are used, i.e., we numerically evaluate the sum of lognormal random variables. Although theoretically, model (b) provides an upper-bound on p_s, we note from the figure that the resulting approximate p_s in model (a) surpasses that obtained by model (b). Consequently, the approximations required for model (a) are not of sufficient accuracy to be used in predicting p_s. For our analysis in log-normal shadowing, we thus employ model (b) which does not rely on any approximations. In [30], [31], Farley proposes an approximation to the CDF of the sum of log-normal random variables, without making any assumption on the distribution of the sum, given by

$$F_Y(y) \approx \left(1 - Q\left(\frac{\log y}{\sigma}\right)\right)^n \quad (28)$$

It is interesting to note that this expression coincides with the CDF of our model (b),

$$\begin{aligned} F_Z(z) &= \text{Prob}(\max_i X_i \le z) = (\text{Prob}(X_i \le z))^n \\ &= \left(1 - Q\left(\frac{\log z}{\sigma}\right)\right)^n \end{aligned} \quad (29)$$

where X_i is log-normally distributed according to Eq. (25).

Fig. 5 shows p_s for several values of the dB spread, as well as for the non-fading case, for $B = 5$ kbps. We observe a similar trend to that of Rayleigh and Ricean fading channels. Since the employed bandwidth is smaller than the bandwidth in Fig. 2, packet collisions are more likely to occur, thus fading provides a greater improvement in p_s than it does in systems with large bandwidths.

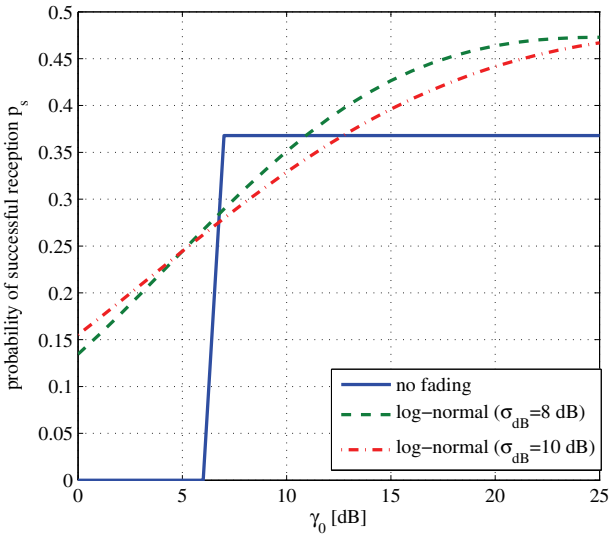

Fig. 5. Probability of successful reception p_s in log-normal shadowing with $B = 5$ kbps. This figure shows that fading improves p_s in both the noise-limited and the interference limited regimes.

V. Network Design Principles

A. Arrival of Useful Packets

We assume that each node generates packets according to independent Poisson processes at an average rate of λ_1 packets per second. Among the successfully received packets, there may be more than one packet corresponding to a single node. Considering that the sensing field has not changed, the extra packets, if successfully received, are redundant. The total number of packets that are used in the reconstruction process, referred to as the *useful packets* and denoted by $K(\lambda_1, T)$, is thus the number of received packets left after discarding the erroneous and repetitive packets at the end of the observation interval T. In a given interval, reconstruction will be successful if sufficiently many useful packets are collected. Otherwise, reconstruction for that particular interval will fail. In what follows we determine the probability distribution of the number of useful packets $K(\lambda_1, T)$.

For a particular node, let $\mathcal{N}_1(T)$ denote the number of packets generated during T that are successfully received. Hence, the number of useful (i.e., successfully received non-repeated) packets generated at each node during T is given by

$$M(T) = \begin{cases} 0, & \mathcal{N}_1(T) = 0 \\ 1, & \mathcal{N}_1(T) \geq 1 \end{cases} \tag{30}$$

The probability of receiving a useful packet from a node is $p_g = \text{Prob}\{M(T) = 1\}$, which can be expressed as

$$\begin{aligned} p_g &= \text{Prob}\{\mathcal{N}_1(T) \geq 1\} \\ &= \sum_{l=1}^{m} \frac{(\lambda_1 T)^l}{l!} e^{-\lambda_1 T}[1 - (1 - p_s)^l] \end{aligned} \tag{31}$$

where each term in the summation is the product of the probability that the node generates l packets during T, and the probability that one or more of the generated packets are successfully received. Note that since a node does not interfere with its own packet, the maximum number of packets that are generated by a single node during T is given by $m = \lfloor \frac{T}{T_p} \rfloor \gg 1$. With this in mind, the expression (31) is approximated as $p_g = 1 - e^{-p_s \lambda_1 T}$.

From (30), the effective average number of packets received from a given node during T is $\overline{M(T)} = p_g$. The average effective arrival rate of useful packets at the FC is thus

$$\lambda' = \frac{N p_g}{T} = \frac{N}{T}(1 - e^{-p_s \lambda_1 T}) \tag{32}$$

where p_s is the probability of successful reception for a given node, determined for various fading conditions in Section IV.

The arrival of useful packets then follows a Poisson process with an effective average arrival rate λ' given by Eq. (32). i.e.,

$$\text{Prob}\{K(\lambda_1, T) = k\} = \frac{(\lambda' T)^k}{k!} e^{-\lambda' T} \tag{33}$$

Using this model, we proceed to determine the sensing rate necessary to achieve a desired performance requirement.

B. Probability of Sufficient Sensing

We define the *probability of sufficient sensing* as the probability that the FC collects N_s or more useful packets during T, and we specify the performance requirement as the minimum probability of sufficient sensing, P_{ss}. Thus,

$$\text{Prob}\{K(\lambda_1, T) \geq N_s\} \geq P_{ss} \tag{34}$$

The condition (34) can equivalently be stated as

$$\alpha \geq \alpha_s \tag{35}$$

where $\alpha = \lambda' T$ represents the average number of useful packets collected in T and is given by

$$\alpha = N(1 - e^{-\lambda_1 T p_s}) \tag{36}$$

and α_s is a design target. Note that p_s is also a function of the per-node sensing rate λ_1. For a given N_s and a desired P_{ss}, one can find the corresponding α_s numerically from Eq. (34). For example, assuming $N = 2500$ and $S = 20$, a required probability of sufficient sensing $P_{ss} = 0.99$ results in $\alpha_s = 355$ packets. Note that we have used $N_s = 2S \log N = 313$ packets, where the value $C = 2$ is determined empirically. Note that the appropriate value of C has to be determined by the system designer, using historical data and/or knowledge of the field and the application (i.e., the tolerable recovery error). In applications of interest to this work (e.g., environmental monitoring), empirical studies using real data and synthetic test cases suggest that a value $C = 2 - 4$ is sufficient for recovery.

C. Design Objective

The design objective is to determine the per-node sensing rate λ_1 that is necessary to ensure sufficient sensing. The condition (35) implies that

$$\lambda_{1s} \leq \lambda_1 \leq \lambda_{1c} \tag{37}$$

where λ_{1s} and λ_{1c} are the solutions to $\alpha = \alpha_s$. We are only interested in those values of λ_1 for which the system is *stable*, i.e., those values for which increasing λ_1 results in

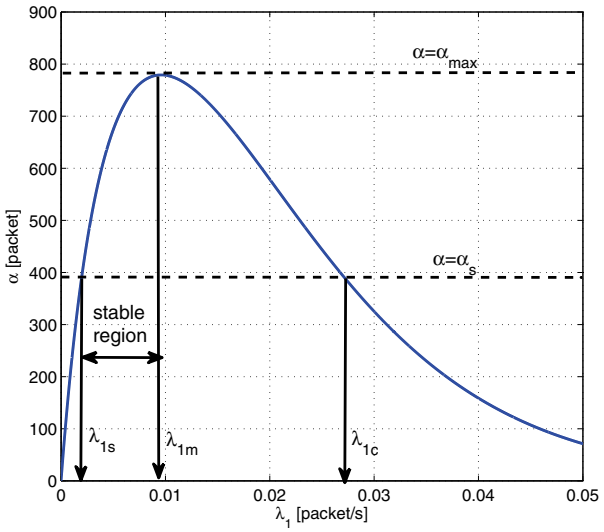

Fig. 6. Average number of useful packets α versus the per-node packet generation rate λ_1. Shown in the figure are λ_{1s} and λ_{1c} (solutions to $\alpha = \alpha_s$) and the region of stability $(\lambda_{1s}, \lambda_{1m})$. Within this region, the desired operating point is near λ_{1s}, which results in the least energy consumption.

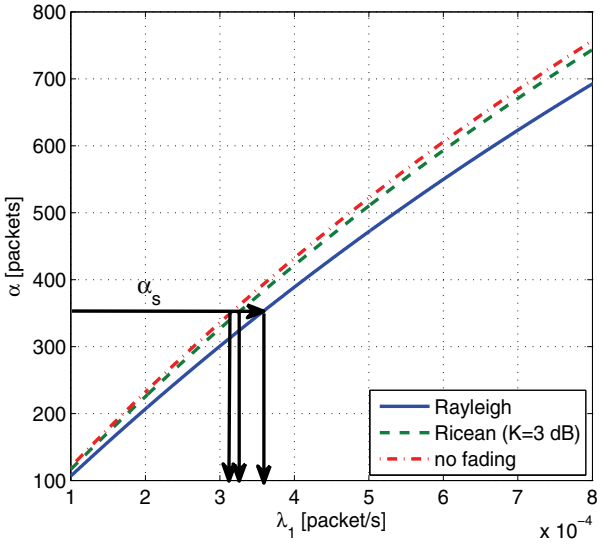

Fig. 7. A required $\alpha_s = 355$ packets, results in a per-node sensing rate $\lambda_{1s} = 3.61 \times 10^{-4}$ for a Rayleigh fading channel, $\lambda_{1s} = 3.3 \times 10^{-4}$ for a Ricean fading channel with $K = 3$ dB, and $\lambda_{1s} = 3.2 \times 10^{-4}$ for a non-fading channel. The rest of the system parameters are $T = 500$ sec, and $B = 38.4$ kbps and $P_{ss} = 0.99$. We notice that for the given parameters the per-node sensing rate is higher in fading.

an increased number of useful packets. Thus the desired value of the per-node sensing rate lies in the stable region

$$\lambda_{1s} \leq \lambda_1 \leq \lambda_{1m} \tag{38}$$

where λ_{1m} is the point at which α reaches its maximum value $\alpha_{\max}$, as noted in Fig. 6. The desired operating point is now chosen to be at the lower edge of the stable region, i.e., at the minimum per-node sensing rate λ_{1s}, since a lower per-node sensing rate corresponds to lower energy consumption, as we will discuss in Section VI.

In a Rayleigh fading channel, using Eq. (23), the per-node sensing rate λ_{1s} can be expressed as

$$\lambda_{1s} = \frac{-1}{2NT_p\beta} \cdot W_0\left(\frac{2NT_p\beta e^{\frac{b}{\gamma_0}}}{T} \log\left(1 - \frac{\alpha_s}{N}\right)\right) \tag{39}$$

where $\beta = b/(b+1)$ and $W_0(\cdot)$ denotes the principal branch of the Lambert W function.[7] In other fading scenarios, λ_{1s} can be determined numerically for a given α_s.

Fig. 7 shows the minimum per-node sensing rate λ_{1s} for Rayleigh, Ricean and non-fading channels. We notice that fading increases the required sensing rate. Note that if a different α_s is required, say because new nodes are introduced into the network, the per-node sensing rate is easily adjusted. Hence, RACS is *scalable*, i.e., it can be tailored to a varying number of nodes.

VI. Bandwidth and Energy Requirements

A. Bandwidth

To achieve a certain sufficient sensing probability, a minimum bandwidth B_s is required. Let us define

$$x_s = \frac{2NT_p\beta e^{b/\gamma_0}}{T} \log\left(1 - \frac{\alpha_s}{N}\right) \tag{40}$$

[7]The Lambert W function $W(x)$ satisfies the equation $W(x)e^{W(x)} = x$ for $x \geq -1/e$. The branch satisfying $W(x) \geq -1$ is denoted by $W_0(x)$.

In order to have a valid solution for λ_{1s}, Eq. (39) implies that $W_0(x_s)$ has to be negative. Thus

$$-1 \leq W_0(x_s) \leq 0 \tag{41}$$

The limit $W_0(x_s) = 0$ in (41) is achieved when $x_s = 0$, or equivalently, when $B \to \infty$. The other limit, $W(x) = -1$, is achieved when $x_s = -1/e$ which corresponds to the minimum bandwidth. The minimum bandwidth B_s in Rayleigh fading is thus obtained in closed form as

$$B_s = \frac{2NL\beta}{T} \cdot e^{(1+b/\gamma_0)} \cdot \log\left(\frac{1}{1 - \alpha_s/N}\right) \tag{42}$$

In other fading conditions B_s can be determined numerically. Now in the non-fading case, for $\gamma_0 \geq b$ we have that

$$B_{s,\text{no fading}} = \frac{2NL}{T} \cdot e \cdot \log\left(\frac{1}{1 - \alpha_s/N}\right) \tag{43}$$

Depending on the choice of the modulation and coding (i.e., the parameter b) and the average received SNR γ_0, fading can lower the bandwidth requirements of RACS. Specifically in Rayleigh fading, if

$$\gamma_0 \geq \frac{b}{\log\left(\frac{b+1}{b}\right)} \tag{44}$$

we observe a saving in the minimum required bandwidth, given by

$$\frac{B_s}{B_{s,\text{no fading}}} = \beta e^{b/\gamma_0} \tag{45}$$

This can be seen from Fig. 8, which shows the minimum required bandwidth in Rayleigh, Ricean and non-fading channels, plotted versus γ_0, for $\gamma_0 > b/\log\left(\frac{b+1}{b}\right)$.

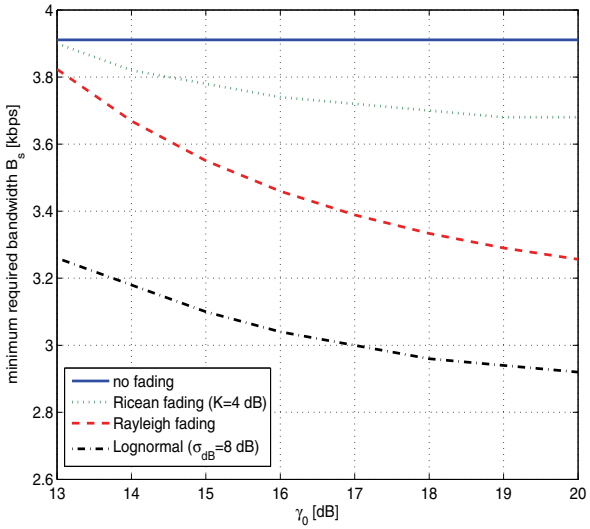

Fig. 8. Minimum bandwidth requirements in Rayleigh, Ricean, Lognormal fading and non-fading channels. System parameters are $T = 500$ sec, $P_{ss} = 0.9$ and $S = 20$. We note that for the moderate and large values of γ_0 fading reduces the required bandwidth.

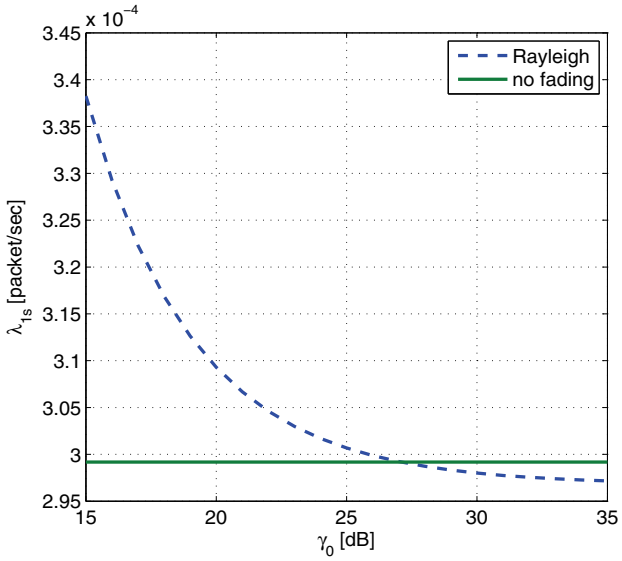

Fig. 9. Minimum required sensing rate λ_{1s} versus γ_0. Increasing γ_0 improves the probability of successful reception in fading (as also observed in Fig. 2) and hence lowers the required sensing rate λ_{1s}. Consequently, in the high-SNR regime, i.e., for $\gamma_0 > 27$ dB, the energy consumption in fading is lower than the energy consumption in non-fading channels.

B. Energy

The total average energy required for one field reconstruction is

$$E = N\lambda_1 T \cdot P_T \cdot T_p \tag{46}$$

where the first term $(N\lambda_1 T)$ is the average number of nodes that transmit in one collection interval T and P_T is the average per-node transmission power. Determining the average transmission power P_T over the entire network in general depends on the geometry of the system and the placement of the nodes. When shadowing is pre-compensated at the transmitter,

$$P_T = P_0 E_{d_i}\{L(d_i)^{-2}\} E_g\{e^{-2g}\} = P_0 \Gamma e^{2\sigma_g^2} \tag{47}$$

where $\Gamma = E_{d_i}\{L(d_i)^{-2}\}$ is the path loss averaged over the nodes' distances to the FC. When shadowing is not compensated,

$$P_T = P_0 \Gamma \tag{48}$$

It is worthwhile to note that in order to maintain a fixed received SNR γ_0, the transmission power P_0 has to scale with the bandwidth, i.e., $P_0 = N_0 B \gamma_0$, resulting in

$$P_T = N_0 B \gamma_0 \cdot \eta \tag{49}$$

where $\eta = \Gamma$ or $\eta = \Gamma e^{2\sigma_g^2}$ depending on whether the lognormal component of the channel is compensated at the transmitter.

For a given bandwidth B, the energy consumption in (46) is minimized if one chooses the minimum sensing rate $\lambda_{1s}(B)$, i.e.,

$$E_{\min}(B) = N\lambda_{1s}(B) T N_0 \gamma_0 \eta L \tag{50}$$

where we have substituted for P_T from Eq. (49). For a fixed bandwidth B, Fig. 9 shows the minimum sensing rate λ_{1s} plotted versus γ_0. We observe that for mid-range γ_0 (i.e., $\gamma_0 = 15 - 27$ dB) the required λ_{1s} in Rayleigh fading is larger than that in a non-fading channel, hence energy consumption is higher. For larger γ_0 (i.e., $\gamma_0 > 27$ dB) the required λ_{1s} is lower in fading, consequently, the energy consumption is lower for this range of γ_0.

The energy expenditure $E_{\min}$ in Eq. (50) depends on the transmission bandwidth B through λ_{1s}. We note that $\lambda_{1s}(B)$ is largest when $B = B_s$ and decreases with B, reaching a limiting value $\lambda_{1s}(\infty)$ as $B \to \infty$. This value is analytically derived as

$$\lambda_{1s}(\infty) = \frac{e^{b/\gamma_0}}{T} \log \frac{1}{1 - \alpha_s/N} \tag{51}$$

The lower and upper bounds on the energy consumption of RACS in Rayleigh fading are thus determined as

$$\begin{aligned} E_{\text{low}} &= \lim_{B\to\infty} E_{\min}(B) \\ &= N N_0 \gamma_0 \eta L \cdot e^{b/\gamma_0} \cdot \log \frac{1}{1 - \alpha_s/N} \end{aligned} \tag{52}$$

and

$$\begin{aligned} E_{\text{up}} &= E_{\min}(B_s) \\ &= N N_0 \gamma_0 \eta L \cdot e^{1+b/\gamma_0} \cdot \log \frac{1}{1 - \alpha_s/N} \end{aligned} \tag{53}$$

We note that the lower and upper bounds are within a constant gap of size e.

C. Savings With Respect to a Benchmark Network

To demonstrate the advantage of the RACS scheme, we compare the energy and bandwidth requirements of RACS with those of a conventional (benchmark) design. The benchmark scheme is a TDMA network in which all N nodes transmit using pre-assigned time slots. The bandwidth and energy requirements of a TDMA network over an ideal communication channel (i.e., no channel fading or noise) are

given by [15]

$$B_{s,TDMA} = \frac{NL}{T} \tag{54}$$

and

$$E_{TDMA} = NT_pP_T = NN_0\gamma_0\eta L \tag{55}$$

In the presence of noise and fading, some of the packets are not successfully received. Let p_f denote the probability of failure for a packet in a TDMA scheme. A common approach to deal with the packet loss is to employ an automatic repeat request (ARQ) scheme, by which the receiver requests retransmission of a failed packet. The average number of retransmissions required to ensure a packet is successfully received is $\frac{1}{1-p_f}$. These retransmissions extend the overall collection interval and require extra transmission energy. Following the outage model, the probability of a failed reception is defined as

$$p_f = \text{Prob}\left\{\frac{X_0}{N_0B} < b\right\} \tag{56}$$

In a Rayleigh fading channel, this probability is given by

$$p_f = 1 - e^{-b/\gamma_0} \tag{57}$$

The bandwidth and energy requirements of the benchmark network using ARQ now increase as

$$B_{s,ARQ} = \frac{NL}{T(1-p_f)} = \frac{NLe^{b/\gamma_0}}{T} \tag{58}$$

and

$$E_{ARQ} = NT_p\frac{P_T}{1-p_f} = NN_0\gamma_0\eta Le^{b/\gamma_0} \tag{59}$$

Under Rayleigh fading, the saving in energy achieved by RACS, over a benchmark network using ARQ is given by

$$G_E = \frac{E_{ARQ}}{E_{\min}(B)} = \frac{e^{b/\gamma_0}}{\lambda_{1s}T} \tag{60}$$

and the saving in bandwidth is given by

$$G_B = \frac{B_{s,ARQ}}{B_s} = \frac{1}{2\beta e\log\frac{1}{1-\alpha_s/N}}. \tag{61}$$

Note that the ARQ scheme is only one viable option to enable reliable data transmission in a sensor network. To ensure reliability of data transfer, few transport layer protocols are proposed in the literature [34], [35]. Rather than individually analyzing each scheme, we note that subjecting the conventional TDMA network to fading and noise inevitably increases the required bandwidth and energy. Thus, we provide a lower bound on the achievable gains by considering a TDMA network in ideal channel conditions (i.e., no fading and no noise).

The lower bound on savings in energy, $G_{E,\text{low}}$, is given by

$$G_{E,\text{low}} = \frac{E_{TDMA}}{E_{\min}(B)} = \frac{1}{\lambda_{1s}T} \tag{62}$$

and the lower bound on savings in bandwidth, $G_{B,\text{low}}$, is given by

$$G_{B,\text{low}} = \frac{B_{s,TDMA}}{B_s} = \frac{1}{2\beta e^{1+b/\gamma_0}\log\frac{1}{1-\alpha_s/N}} \tag{63}$$

Fig. 10 shows these savings achieved over the benchmark scheme. We notice that considerable gain in energy– on the order of 20 dB– is achievable. Also, we observe a reduction in the required bandwidth, say 20 fold decrease in the bandwidth for a network of size $N = 4 \times 10^4$.

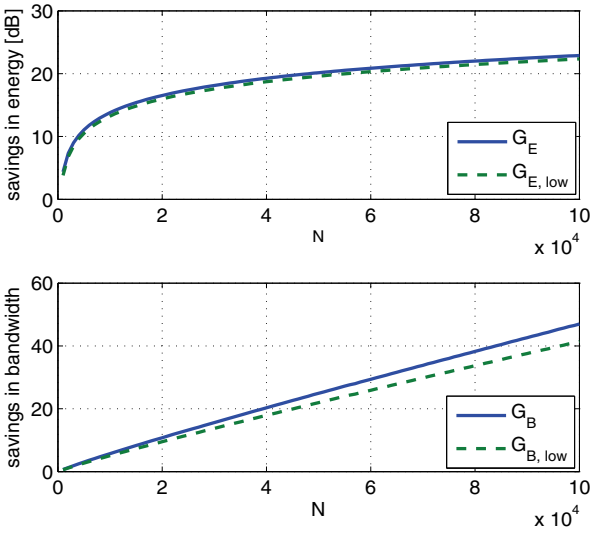

Fig. 10. Savings in energy and bandwidth achieved using RACS (in Rayleigh fading) over a benchmark TDMA scheme. System parameters are $T = 500$ sec, the probability of sufficient sensing $P_{ss} = 0.9$, and $\gamma_0 = 15$ dB. The sparsity is assumed to be fixed at $S = 20$.

VII. Conclusion

RACS is an integrated sensing and communication architecture that combines the concepts of random channel access and compressed sensing to achieve energy and bandwidth efficiency. To address realistic deployments conditions, we took into consideration the impact of channel fading and noise on the design and performance of a RACS network. We provided analytical expressions for the minimum bandwidth needed to support the RACS network, as well as the bounds on its energy consumption. For the practical range of the SNR, say 15-25 dB, the minimum required bandwidth in a fading channel is lower than in a non-fading channel; however, the energy consumption is higher in fading. More importantly, it was shown that RACS achieves considerable energy and bandwidth gains over a benchmark TDMA network.

In addition to energy and bandwidth efficiency, RACS affords scalability and robustness against random (isolated) node failures, since the loss of a packet at random bears no consequence on the random nature of the packet arrival process. These features constitute an attractive scheme for large scale wireless sensor networks, deployed for long term monitoring of sparse phenomena (e.g., environmental monitoring).

Appendix A

The probability distribution of X_0 and I_n are given by f_X and f_I, respectively, where

$$f_I = \begin{cases} f_Y & \text{for } I_n = Y_n \\ f_M & \text{for } I_n = M_n \end{cases} \tag{64}$$

We define two new random variables $\gamma = \frac{X_0}{I_n+N_0B}$ and $w = I_n + N_0B$. We have that

$$f_{\gamma,w}(\gamma, w) = f_{X_0,I_n}(\gamma w, w - N_0B).|J| \tag{65}$$

where J is the Jacobian of the transformation

$$J = \begin{Vmatrix} \frac{\partial X_0}{\partial \gamma} & \frac{\partial X_0}{\partial w} \\ \frac{\partial I_n}{\partial \gamma} & \frac{\partial I_n}{\partial w} \end{Vmatrix} \tag{66}$$

The joint probability distribution of γ and w is now given by

$$f_{\gamma,w}(\gamma, w) = f_X(\gamma w) f_I(w - N_0B) w \tag{67}$$

The pdf of γ is then obtained as

$$f_\gamma(\gamma) = \int_{N_0B}^{\infty} f_{\gamma,w}(\gamma, w) dw \tag{68}$$

Now averaging $p_{s|n}(\gamma)$ in Eq. (15) over the statistics of γ, we have that

$$p_{s|n} = \begin{cases} \int_{bN_0B}^{\infty} f_X(x)dx & \text{for } n = 0 \\ \int_b^{\infty}\int_{N_0B}^{\infty} f_X(\gamma w) f_I(w - N_0B) w dw d\gamma & \text{for } n \geq 1 \end{cases} \tag{69}$$

APPENDIX B

The distribution of the power of the received signal X_0 in Ricean fading is a non-central χ^2 with 2 degrees of freedom [36] given by

$$f_X(x) = \frac{1+K}{P_0} \cdot e^{-K-\frac{x(1+K)}{P_0}} \cdot I_0\left[2\sqrt{\frac{xK(1+K)}{P_0}}\right] \tag{70}$$

The pdf of Y_n is a non-central χ^2 random variable with $2n$ degrees of freedom given by

$$f_Y(y) = \left(\frac{1+K}{P_0}\right)^{\frac{n+1}{2}} \left(\frac{y}{nK}\right)^{\frac{n-1}{2}} e^{-nK-\frac{y(1+K)}{P_0}} I_{n-1}\left(2\sqrt{\frac{(1+K)nKy}{P_0}}\right) \tag{71}$$

where $I_{n-1}(\cdot)$ is the $(n-1)$-order modified Bessel function of the first kind. Finally,

$$f_M(z) = n\left(1 - Q_1\left(\sqrt{2K}, \sqrt{\frac{2(1+K)z}{P_0}}\right)\right)^{n-1} \frac{1+K}{P_0} \cdot e^{-K-\frac{z(1+K)}{P_0}} \cdot I_0\left(2\sqrt{\frac{zK(1+K)}{P_0}}\right). \tag{72}$$

REFERENCES

[1] J. K. Hart and K. Martinez, "Environmental sensor networks: a revolution in the earth system science?" *Earth-Science Rev.*, vol. 78, pp. 177–191, 2006.

[2] E. M. Sozer, M. Stojanovic, and J. G. Proakis, "Underwater acoustic networks," *IEEE J. Oceanic Eng.*, vol. 25, no. 1, pp. 72–83, Jan. 2000.

[3] G. Werner-Allen, J. Johnson, M. Ruiz, J. Lees, and M. Welsh, "Monitoring volcanic eruptions with a wireless sensor network," in *2005 European Workshop Wireless Sensor Netw.*

[4] K. Martinez, P. Padhy, A. Elsaify, G. Zou, A. Riddoch, J. Hart, and H. Ong, "Deploying a sensor network in an extreme environment," in *2006 IEEE International Conf. Sensor Netw., Ubiquitous Trustworthy Comput.*

[5] W. Bajwa, J. Haupt, A. Sayeed, and R. Nowak, "Compressive wireless sensing," in *Proc. 2006 Int. Conf. Inf. Process. Sensor Netw.*, pp. 134–142.

[6] W. Bajwa, A. Sayeed, and R. Nowak, "Matched source-channel communication for field estimation in wireless sensor networks," in *Proc. 2005 Int. Conf. Inf. Process. Sensor Netw.*, pp. 332–339.

[7] W. Bajwa, J. Haupt, A. Sayeed, and R. Nowak, "Joint source-channel communication for distributed estimation in sensor networks," *IEEE Trans. Inf. Theory*, vol. 53, no. 10, pp. 3629–3653, Oct. 2007.

[8] J. Meng, H. Li, and Z. Han, "Sparse event detection in wireless sensor networks using compressive sensing," in *Proc. 2009 Conf. Inf. Sciences Syst.*, pp. 181–185.

[9] A. Griffin and P. Tsakalides, "Compressed sensing of audio signals using multiple sensors," in *Proc. 2008 European Signal Process. Conf.*

[10] C. Luo, F. Wu, J. Sun, and C. W. Chen, "Compressive data gathering for large-scale wireless sensor networks," in *Proc. 2009 International Conf. Mobile Comput. Netw.*, pp. 145–156.

[11] C. T. Chou, R. Rana, and W. Hu, "Energy efficient information collection in wireless sensor networks using adaptive compressive sensing," in *Proc. 2009 IEEE Conf. Local Comput. Netw.*, pp. 443–450.

[12] R. Masiero, G. Quer, D. Munaretto, M. Rossi, J. Widmer, and M. Zorzi, "Data acquisition through joint compressive sensing and principal component analysis," in *Proc. 2009 IEEE Conf. Global Telecommun.*, pp. 1271–1276.

[13] R. Masiero, G. Quer, M. Rossi, and M. Zorzi, "A Bayesian analysis of compressive sensing data recovery in wireless sensor networks," in *Proc. 2009 ICUMT*, pp. 1–6.

[14] S. Lee, S. Pattem, M. Sathiamoorthy, B. Krishnamachari, and A. Ortega, "Spatially-localized compressed sensing and routing in multi-hop sensor networks," in *GeoSensor Netw.*, ser. Lecture Notes in Comput. Science. Springer, 2009, pp. 11–20.

[15] F. Fazel, M. Fazel, and M. Stojanovic, "Compressed sensing in random access networks with applications to underwater monitoring," *Physical Commun. J.*, vol. 5, no. 2, June 2012.

[16] ——, "Random access compressed sensing for energy-efficient underwater sensor networks," *IEEE J. Sel. Areas Commun.*, vol. 29, no. 8, Sept. 2011.

[17] E. J. Candes, J. Romberg, and T. Tao, "Robust uncertainty principles: exact signal reconstruction from highly incomplete frequency information," *IEEE Trans. Inf. Theory*, vol. 52, pp. 489–509, Mar. 2006.

[18] E. Candes and J. Romberg, "Sparsity and incoherence in compressive sampling," *Inverse Problems*, vol. 23, pp. 969–985, 2007.

[19] E. J. Candes and M. B. Wakin, "An introduction to compressive sampling," *IEEE Signal Process. Mag.*, pp. 21–30, Mar. 2008.

[20] K. R. Rao, D. N. Kim, and J. J. Hwang, "Nonuniform DFT," in *Fast Fourier Transform - Algorithms and Applications*, ser. Signals Commun. Technol. Springer, 2011, pp. 195–234.

[21] F. Fazel, M. Fazel, and M. Stojanovic, "Design of a random access network for compressed sensing," in *2011 Inf. Theory Appl.*

[22] L. G. Roberts, "Aloha packet system with and without slots and capture," *SIGCOMM Comput. Commun. Rev.*, vol. 5, pp. 28–42, Apr. 1975.

[23] M. Schwartz, *Mobile Wireless Communications*. Cambridge University Press, 2005.

[24] J. Linnartz, *Narrowband Land-Mobile Radio Networks*. Artech House, Inc., 1993.

[25] M. Zorzi and S. Pupolin, "Outage probability in multiple access packet radio networks in the presence of fading," *IEEE Trans. Veh. Technol.*, vol. 43, no. 3, pp. 1–6, Aug. 1994.

[26] M. K. Simon and M. Alouini, *Digital Communication over Fading Channels*. John Wiley & Sons, 2005.

[27] H. Suzuki, "A statistical model for urban radio propagation," *IEEE Trans. Commun.*, vol. COM-25, no. 7, pp. 673–680, July 1977.

[28] F. Fazel, M. Fazel, and M. Stojanovic, "Impact of fading on random access compressed sensing," in *2011 Asilomar Conf. Signals, Syst., Comput.*

[29] M. Marsan, G. Hess, and S. Gilbert, "Shadowing variability in an urban land mobile environment at 900 MHz," *Electron. Lett.*, vol. 26, no. 10, pp. 646–648, May 1990.

[30] N. C. Beaulieu, A. A. Abu-Dayya, and P. J. McLane, "Estimating the distribution of a sum of independent lognormal random variables," *IEEE Trans. Commun.*, vol. 43, no. 12, Dec. 1995.

[31] S. C. Schwartz and Y. S. Yeh, "On the distribution function and moments of power sums with log-normal components," *Bell Syst. Tech. J.*, vol. 61, no. 7, Sept. 1982.

[32] L. F. Fenton, "The sum of log-nomral probability distributions in scatter transmission systems," *IRE Trans. Commun. Syst.*, vol. 8, Mar. 1960.

[33] P. Cardieri and T. S. Rappaport, "Statistics of the sum of lognormal variables in wireless communication," in *2000 Veh. Technol. Conf.*

[34] P. R. Pereira, A. Grilo, F. Rocha, M. S. Nunes, A. Casaca, C. Chaudet, P. Almstrom, and M. Johansson, "End-to-end reliability in wireless sensor networks: survey and research challenges," in *2007 EuroFGI Workshop IP QoS Traffic Control*.
[35] J. Yick, B. Mukherjee, and D. Ghosal, "Wireless sensor network survey," *Comput. Netw.*, vol. 52, no. 2292-2330, Aug. 2008.
[36] J. G. Proakis, *Digital Communications*, 3rd edition. McGraw Hill, 1995.

Fatemeh Fazel received her B.Sc. degree from Sharif University, Tehran, Iran, her M.Sc. degree from University of Southern California, and her Ph.D. degree from the University of California, Irvine, all in electrical engineering. She is currently an associate research scientist in the electrical and computer engineering department at Northeastern University, Boston. Her research interests are in signal processing methods for wireless communications and sensor networks.

Maryam Fazel received her BS degree from Sharif University, Iran, and her MS and PhD degrees from Stanford University in 2002. She was a postdoctoral scholar and later a Research Scientist in the Control and Dynamical Systems Department at Caltech until 2007. She is currently an assistant professor in the Electrical Engineering Department at the University of Washington, Seattle, with adjunct appointments in Mathematics and in Computer Science and Engineering. She is the recipient of a 2009 NSF CAREER Award and an Outstanding Teaching Award at the University of Washington.

Milica Stojanovic (Sm'08,F'10) graduated from the University of Belgrade, Serbia, in 1988, and received the M.S. and Ph.D. degrees in electrical engineering from Northeastern University, Boston, MA, in 1991 and 1993. After a number of years with the Massachusetts Institute of Technology, where she was a Principal Scientist, she joined the faculty of Electrical and Computer Engineering Department at Northeastern University in 2008. She is also a Guest Investigator at the Woods Hole Oceanographic Institution, and a Visiting Scientist at MIT. Her research interests include digital communications theory, statistical signal processing and wireless networks, and their applications to underwater acoustic communication systems. Milica is an Associate Editor for the *IEEE Journal of Oceanic Engineering* and the IEEE TRANSACTIONS ON SIGNAL PROCESSING.